Surface Gravity and Capillary Waves☆☆

Yusuke Uchiyama, Kobe University, Kobe, Japan

© 2018.

Introduction

Ocean surface waves are the most common oceanographic phenomena that are known to the casual observer. They can at once be the source of inspiration and primal fear. It is remarkable that the complex, random wave field of a storm-lashed sea can be studied and modeled using well-developed theoretical concepts. Many of these concepts are based on linear or weakly nonlinear approximations to the full nonlinear dynamics of ocean waves. Early contributors to these theories included such luminaries as Cauchy, Poisson, Stokes, Lagrange, Airy, Kelvin, and Rayleigh. Many of the current challenges in the study of ocean surface waves are related to nonlinear processes that have not been well understood yet. These include dynamical coupling between the atmosphere and the ocean, wave–wave interactions, and wave breaking.

For the purposes of this article, surface waves are considered to extend from low frequency swell from distant storms at periods of 10 s or more and wavelengths of hundreds of meters, to capillary waves with wavelengths of millimeters and frequencies of $O(10)$ Hz. In between are wind waves with lengths of $O(1-100)$ m and periods of $O(1-10)$ s. **Fig. 1** shows a spectrum of surface waves measured from the Research Platform FLIP off the coast of Oregon. The spectrum, Φ, shows the distribution of energy in the wave field as a function of frequency. The wind wave peak at approximately 0.13 Hz is well separated from the swell peak at approximately 0.06 Hz.

Ocean surface waves play an important role in air–sea interaction. Momentum from the wind goes into both surface waves and currents. Ultimately the waves are dissipated either by viscosity or breaking, giving up their momentum to currents. Surface waves affect upper-ocean mixing through both wave breaking and their role in the generation of Langmuir circulations. This breaking and mixing influence the temperature of the ocean surface and thus the thermodynamics of air–sea interaction. Surface waves impose significant structural loads on ships and other structures. Remote sensing of the ocean surface, from local to global scales, depends on the surface wave field.

Basic Formulations

The dynamics and kinematics of surface waves are described by solutions of the Navier–Stokes equations for an incompressible viscous fluid, with appropriate boundary and initial conditions. Surface waves of the scale described here are usually generated by the wind, so the complete problem would include the dynamics of both the water and the air above. However, the density of the air is approximately 800 times smaller than that of the water, so many aspects of surface wave kinematics and dynamics may be considered without invoking dynamical coupling with the air above.

The influence of viscosity is represented by the Reynolds number of the flow, $R_e = UL/\nu$, where U is a characteristic velocity, L a characteristic length scale, and $\nu = \mu/\rho$ is the kinematic viscosity, where μ is the viscosity and ρ the density of the fluid. The Reynolds number is the ratio of inertial forces to viscous forces in the fluid and if $R_e \gg 1$, the effects of viscosity are often confined to thin boundary layers, with the interior of the fluid remaining essentially inviscid ($\nu = \mu = 0$) by assuming a homogeneous fluid. In contrast, internal waves in stratified fluids are rotational since they introduce baroclinic generation of vorticity in the interior of the fluid. Denoting the fluid velocity by $\mathbf{u} = (u, v, w)$, the vorticity of the flow is given by $\zeta = \nabla \times \mathbf{u}$. If $\zeta = 0$, the flow is said to be irrotational. From Kelvin's circulation theorem, the

---
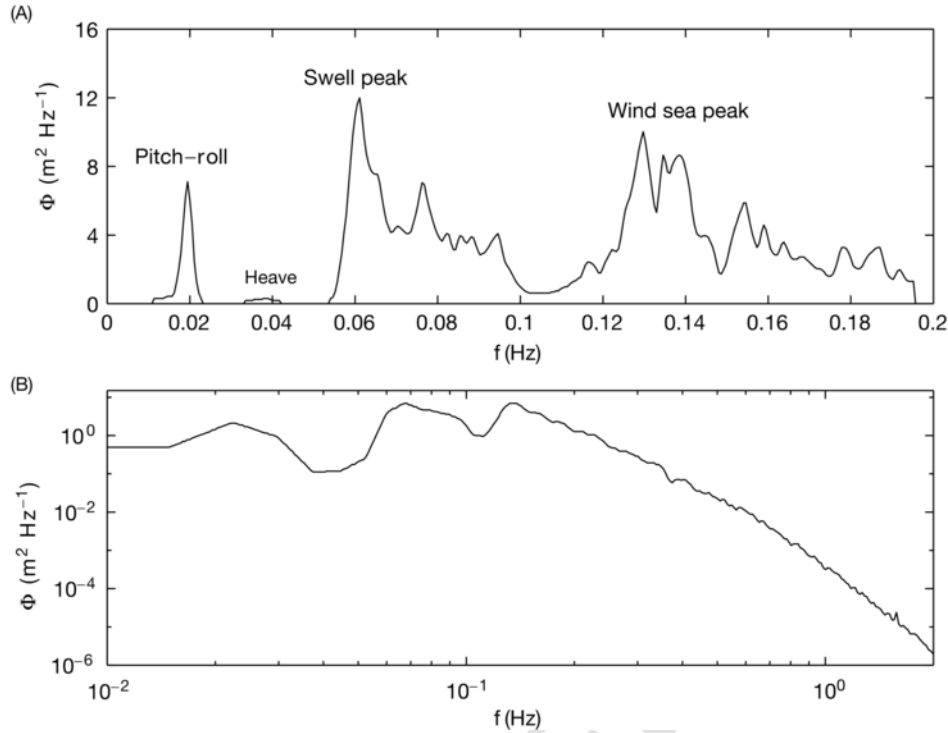
Fig. 1 (A) Surface displacement spectrum measured with an electromechanical wave gauge from the Research Platform FLIP in 8 m s^{-1} winds off the coast of Oregon. Note the wind-wave peak at 0.13 Hz, the swell at 0.06 Hz and the heave and pitch and roll of FLIP at 0.04 and 0.02 Hz respectively. (B) An extension of (A) with logarithmic spectral scale, note that from the wind sea peak to approximately 1 Hz the spectrum has a slope like f^{-4}, common in wind-wave spectra. Reproduced with permission from Felizardo, F. C. and Melville, W. K. (1995). Correlations between ambient noise and the ocean surface wave field. *Journal of Physical Oceanography* **25**, 513–532.

irrotational flow of an incompressible ($\nabla \cdot \mathbf{u} = 0$) inviscid fluid will remain irrotational as the flow evolves. The essential features of surface waves may be considered in the context of incompressible irrotational flows.

For an irrotational flow, a scalar velocity potential ϕ can be introduced, so that $\mathbf{u} = \nabla \phi$. Then, by virtue of incompressibility, ϕ satisfies Laplace's equation

$$\nabla^2 \phi = 0 \tag{1}$$

from the incompressible continuity. We denote the surface by $z = \eta(x, y, t)$, where (x, y) are the horizontal coordinates, z is the vertical coordinate, and t is time. The kinematic condition at the impermeable bottom at $z = -h$, is one of no flow through the boundary:

$$\frac{\partial \phi}{\partial z} = 0 \ \text{ at } \ z = -h \tag{2}$$

There are two boundary conditions at $z = \eta$:

$$\frac{\partial \eta}{\partial t} + u \frac{\partial \eta}{\partial x} + v \frac{\partial \eta}{\partial y} = w \tag{3}$$

$$\frac{\partial \phi}{\partial t} + \frac{1}{2} \mathbf{u}^2 + g\eta = \left(p_a - p \right) / \rho \tag{4}$$

The first is a kinematic condition, which is equivalent to imposing the condition that elements of fluid at the surface remain at the surface. The second is a dynamical condition, a Bernoulli equation, which is equivalent to stating that the pressure p_- at $z = \eta_-$, an infinitesimal distance beneath the surface, is just a constant atmospheric pressure, p_a, plus a contribution from surface tension. The effect of gravity is to impose a restoring force tending to bring the surface back to $z = 0$. The effect of surface tension is to reduce the curvature of the surface.

Although this formulation of surface waves is considerably simplified already, there are profound difficulties in predicting the evolution of surface waves based on these equations. Although Laplace's equation is linear, the surface boundary conditions are nonlinear and apply on a surface whose specification is a part of the solution. Our ability to accurately predict the evolution of nonlinear waves is limited and largely dependent on numerical techniques. The usual practice is to linearize the boundary conditions about $z = 0$.

Linear Waves

Simple harmonic surface waves are characterized by an amplitude a, half the distance between the crests and the troughs, and a wavenumber vector $\mathbf{k}$ with $|\mathbf{k}| = k = 2\pi/\lambda$, where λ is the wavelength. The surface displacement is

$$\eta = a e^{i(\mathbf{k}.\mathbf{x} - \sigma t)} \tag{5}$$

where $\sigma = 2\pi/T$ is the radian frequency, $\mathbf{x} = (x, y)$, and T is the wave period. Then ak is a measure of the slope of the waves, and if $ak \ll 1$, the surface boundary conditions can be linearized about $z = 0$. Unless otherwise stated, the real part of complex expressions is taken to obtain solutions.

Following linearization, the boundary conditions become

$$\frac{\partial \eta}{\partial t} = w \tag{6}$$

$$\frac{\partial \phi}{\partial t} + g\eta = \frac{\Gamma}{\rho} \left(\frac{\partial^2 \eta}{\partial x^2} + \frac{\partial^2 \eta}{\partial y^2} \right) \quad \text{at} \quad z = 0 \tag{7}$$

where the linearized Laplace pressure is

$$p_a - p_- = \Gamma \left(\frac{\partial^2 \eta}{\partial x^2} + \frac{\partial^2 \eta}{\partial y^2} \right) \tag{8}$$

and Γ is the surface tension coefficient.

Substituting for η and satisfying Laplace's equation and the boundary conditions at $z = 0$ and $-h$ gives

$$\phi = \frac{ig'a \cosh k\,(z + h)}{\sigma \cosh kh}, \tag{9}$$

where

$$\sigma^2 = g'k \tanh kh \tag{10}$$

and

$$g' = g \left(1 + \Gamma k^2/\rho \right) \tag{11}$$

which is effective gravity modified by surface tension. Equations relating the frequency and wavenumber, $\sigma = \sigma(k)$, are known as dispersion relations, and for linear waves provide a fundamental description of the wave kinematics. If surface tension is negligible, $\Gamma \ll 1$ and $g' \to g$, then dispersion relation **(10)** becomes $\sigma^2 = gk \tanh kh$. The phase speed,

$$c = \sigma/k = \left(\frac{g'}{k} \tanh kh \right)^{1/2} \tag{12}$$

is the speed at which lines of constant phase (e.g., wave crests) move.

For waves propagating in the x-direction, the velocity field is

$$u = \frac{g'ak}{\sigma} \frac{\cosh(z + h)}{\cosh kh} e^{i(kx - \sigma t)} \tag{13}$$

$$v = 0 \tag{14}$$

$$w = \frac{ig'ak}{\sigma} \frac{\sinh(z+h)}{\cosh kh} e^{i(kx-\sigma t)} \tag{15}$$

and the pressure is

$$p = \rho g' \eta \frac{\cosh(z+h)}{\cosh kh} \tag{16}$$

where the hydrostatic pressure is subtracted. The velocity decays with depth away from the surface, and, to leading order, elements of fluid execute elliptical orbits as the waves propagate.

For shallow water, $kh \ll 1$,

$$(u, v, w, p) = \left(\frac{g'k}{\sigma}, 0, 0, \rho g' \right) \eta \tag{17}$$

so that there is no vertical motion, just a uniform sloshing back and forth in the horizontal plane in phase with the surface displacement η. The phase speed $c = (g'h)^{1/2}$, is independent of the wavenumber. Such waves are said to be nondispersive. Waves propagating toward shore eventually attain this condition, and, as the depth tends to zero, nonlinear effects become important as ak increases.

For very deep water, $kh \gg 1$,

$$(u, v, w, p) = \left(\frac{g'k}{\sigma}, 0, -\frac{ig'k}{\sigma}, \rho g' \right) e^{kz} \eta \tag{18}$$

so that the water particles execute circular motions that decay exponentially with depth. The horizontal motion is in phase with the surface displacement, and the phase speed of the waves

$$c = \left(g'/k \right)^{1/2} = \left[\frac{g}{k} \left(1 + \Gamma k^2 / \rho g \right) \right]^{1/2} \tag{19}$$

These deep-water waves are dispersive; that is, the phase speed is a function of the wavenumber as shown in **Fig. 2**. The influence of surface tension relative to gravity is determined by the value of the dimensionless parameter $\Sigma = \Gamma k^2 / \rho g$. When $\Sigma = 1$, the wavelength $\lambda = 1.7$ cm and the phase speed is a minimum at $c = 23$ cm s^{-1}. When $\Sigma \gg 1$, surface tension is the dominant restoring force over gravity,   the
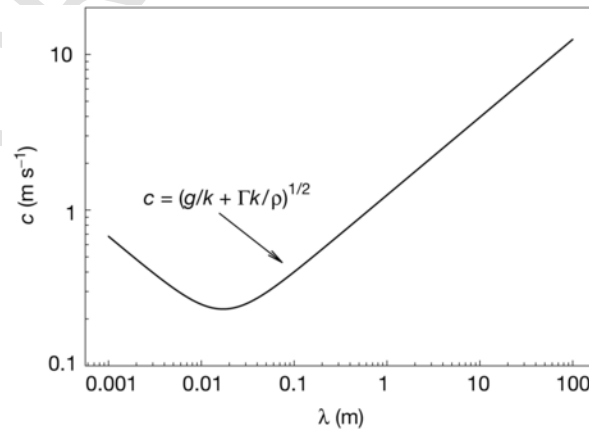
Fig. 2   The phase speed of surface gravity-capillary waves as a function of wavelength λ. A minimum phase speed of 23 cm s^{-1} occurs for $\lambda = 0.017$ m. Shorter waves approach pure capillary waves, whereas longer waves become pure gravity waves. Note that there are both capillary and gravity waves for a given phase speed. This is the basis of the generation of parasitic capillary waves on the forward face of steep gravity waves.

wavelength is less than 1.7 cm, and the phase speed increases as the wavelength decreases. When $\Sigma \ll 1$, gravity is the dominant restoring force over surface tension, the wavelength is greater than 1.7 cm, and the phase speed increases as the wavelength increases.

The Group Velocity

Using the superposition principle over a continuum of wavenumbers a general disturbance (in two spatial dimensions) can be represented by

$$\eta(x,t) = \int_{-\infty}^{\infty} a(k) e^{i(kx-\sigma t)} dk \tag{20}$$

where, as above, only the real part of the integral is taken. Assuming the disturbance is confined to wavenumbers in the neighborhood of k_o, and expanding $\sigma(k)$ about k_o gives

$$\sigma(k) = \sigma(k_o) + (k - k_o) \frac{d\sigma}{dk}\Big|_{k=k_0} + \dots \tag{21}$$

whence

$$\eta(x,t) \doteq e^{i(k_o x - \sigma(k_o)t)} \int_{-\infty}^{\infty} a(k) e^{i(k-k_o)(x-c_g t)} dk + \dots \tag{22}$$

where

$$c_g = \left|\frac{d\sigma}{dk}\right|_{k=k_0} = \frac{c}{2}\left(1 + \frac{2kh}{\sinh 2kh}\right) \tag{23}$$

is the group velocity. Eq. **(22)** demonstrates that the modulation of the pure harmonic wave propagates at the group velocity. This implies that an isolated packet of waves centered around the wavenumber k_o will propagate at the speed c_g, so that an observer wishing to follow waves of the same length must travel at the group velocity. Since the energy density is proportional to a^2 (see below), it is also the speed at which the energy propagates. These properties of the group velocity apply to linear waves, and more subtle effects may become important at large slopes. From Eq. **(23)**, $c_g \neq c$ in general.

For deep-water gravity waves, $kh \gg 1$,

$$c_g = \frac{1}{2}c = \frac{1}{2}\left(\frac{g}{k}\right)^{1/2} \tag{24}$$

so the wave group travels at half the phase speed, with waves appearing at the rear of a group propagating forward and disappearing at the front of the group.

For deep-water capillary waves,

$$\sigma^2 = \Gamma k^3/\rho, c = (\Gamma k/\rho)^{1/2}, c_g = \frac{3}{2}c \tag{25}$$

so waves appear at the front of the group and disappear at the rear of the group as it propagates.

For shallow water gravity waves, $kh \ll 1$, $c_g = c$.

Second Order Quantities

The energy density (per horizontal surface area) of surface waves is

$$E = \frac{1}{2}\rho g' a^2 \tag{26}$$

being the sum of the kinetic and potential energies. In the case of gravity waves, the potential energy results from the displacement of the surface about its equilibrium horizontal position. For capillary waves, the potential energy arises from the stretching of the surface against the restoring force of surface tension.

The mean momentum density **M** is given by

$$\mathbf{M} = \frac{1}{2}\rho\sigma a^2 \coth kh \cdot \frac{\mathbf{k}}{k} = \frac{E}{c} \cdot \frac{\mathbf{k}}{k} \tag{27}$$

To leading order, linear gravity waves transfer energy without transporting mass; however, there is a second order mass transport associated with surface waves. In a Lagrangian description of the flow it can be shown that for irrotational inviscid wave motion the mean horizontal Lagrangian velocity (Stokes drift), $\mathbf{u}^{st}$, of a particle of fluid originally at $z = z_o$ is

$$\mathbf{u}^{st} = \sigma k a^2 \frac{\cosh 2k\,(z+h)}{2\sinh^2 kh} \cdot \frac{\mathbf{k}}{k} \tag{28}$$

which reduces to $(ak)^2\, ce^{2kz}{}_o\, \mathbf{k}/k$ when $kh \gg 1$. This second order velocity arises from the fact that the orbits of the particles of fluid are not closed. Integrating Eq. **(28)** over the depth it can be shown that this mean Lagrangian velocity accounts for the wave momentum **M** in the Eulerian description. The Stokes drift is important for representing scalar transport near the ocean surface, but this transport is likely to be significantly enhanced by the intermittent larger velocities associated with wave breaking.

Longer waves, or swell, from distant storms can travel great distances. An extreme example is the propagation of swell along great circle routes from storms in the Southern Ocean to the coast of California. For waves to travel so far, the effects of dissipation must be small. In deep water, where the wave motions have decayed away to negligible levels at depth, the contributions to the dissipation come from the thin surface boundary layer and the rate of strain of the irrotational motions in the bulk of the fluid. It can be shown that the integral is dominated by the latter contributions, and the timescale for the decay of the wave energy is just

$$\tau_e = -\left(\frac{1}{E}\frac{dE}{dt}\right)^{-1} = \left(4\nu k^2\right)^{-1} \tag{29}$$

or $\sigma/8\pi\nu k^2$ wave periods. This gives negligible dissipation for long-period swell in deep water over scales of the ocean basins. More realistic models of wave dissipation must take into account breaking and near surface turbulence, sometimes parameterized as an eddy viscosity, which is several orders of magnitude greater than the molecular viscosity. When waves propagate into shallow water, the dominant dissipation may occur in the bottom boundary layer.

Eq. **(27)** shows that dissipation of wave energy is concomitant with a reduction in wave momentum, but since momentum is conserved, the reduction of wave momentum is accompanied by a transfer of momentum from waves to currents. That is, net dissipative processes in the wave field lead to the generation of currents.

Waves on Currents: Action Conservation

Waves propagating in varying currents may exchange energy with the current, thus modifying the waves. Perhaps the most dramatic examples of this effect come when waves propagating against a current become larger and steeper. Examples occur off the east coast of South Africa as waves from the Southern Ocean meet the Aghulas Current; as North Atlantic storms meet the northward flowing Gulf Stream, or at the mouths of estuaries as shoreward propagating waves meet the ebb tide.

For currents $\mathbf{U} = (U, V)$ that only change slowly on the scale of the wavelength, and a surface displacement of the form

$$\eta = a\,(x, y, t)\, e^{i\theta(x,y,t)} \tag{30}$$

where a is the slowly varying amplitude and θ is the phase. The absolute local frequency $\omega = -\partial\theta/\partial t$, and the x- and y-components of the local wavenumber are given by $k = \partial\theta/\partial x$, $l = \partial\theta/\partial y$. The frequency seen by an observer moving with the current **U** is

$$-\left(\frac{\partial\theta}{\partial t} + \mathbf{U}.\nabla\theta\right) \tag{31}$$

which is equal to the intrinsic frequency σ. Thus we obtain

$$\sigma = \omega - \mathbf{U}.\mathbf{k} \tag{32}$$

the Doppler relationship. This frequency Doppler shifting leads to modification of dispersion relation **(10)**.

We also have conservation of wavenumber **k** rearranged in the following form:

$$\frac{\partial \mathbf{k}}{\partial t} + \nabla \omega = 0 \tag{33}$$

which can be interpreted as the conservation of wave crests, where **k** is the spatial density of crests and ω the wave flux.

The velocity of a wave packet along rays is

$$\frac{dx_i}{dt} = U_i + \frac{\partial \sigma}{\partial x_i} = U_i + c_{gi} \tag{34}$$

which is simply the vector sum of the local current and the group velocity in a fluid at rest. Furthermore, refraction is governed by

$$\frac{\mathrm{d} k_i}{\mathrm{d} t} = -k_j \frac{\partial U_j}{\partial x_i} - \frac{\partial \sigma}{\partial x_i} \tag{35}$$

where the first term on the right represents refraction due to the current and the second is due to gradients in the waveguide, such as changes in the depth. It is this latter term that results in waves, propagating from deep water toward a beach, refracting so that they propagate normal to shore.

For steady currents, the absolute frequency is constant along rays but the intrinsic frequency may vary, and the dynamics lead to a remarkable and quite general result for linear waves. If E is the energy density then the quantity $\mathscr{A} = E/\sigma$, the wave action, is conserved:

$$\frac{\partial \mathscr{A}}{\partial t} + \frac{\partial}{\partial x_i} \left[\left(U_i + c_{gi} \right) \mathscr{A} \right] = 0 \tag{36}$$

In other words, the variations in the intrinsic frequency σ and the energy density E, are such as to conserve the quotient.

This theory permits the prediction of the change of wave properties as they propagate into varying currents and water depths. For example, in the case of waves approaching an increasing counter current, the waves will move to shorter wavelengths (higher k), larger amplitudes, and hence greater slopes, ak. As the speed of the adverse current approaches the group velocity, the waves will be "blocked" and be unable to propagate further. In this simplest theory, a singularity occurs with the wave slope becoming infinite, but higher order effects lead to reflection of the waves and the same blocking effect. This theory also forms the basis of models of long-wave–short-wave interaction that are important for wind-wave generation and the interpretation of remote sensing measurements of the ocean surface, including the remote sensing of long nonlinear internal waves.

Nonlinear Effects

The nonlinearity of surface waves is represented by the wave slope, ak. For typical gravity waves at the ocean surface the average slope may be $O(10^{-2} - 10^{-1})$; small, but not negligibly so. Nonlinear effects may be weak and can be described as a perturbation to the linear wave theory, using the slope as an expansion parameter. This approach, pioneered by Stokes in the mid-19th century, showed that for uniform approach deep-water gravity waves,

$$\sigma^2 = gk \left(1 + a^2 k^2 + \dots \right) \tag{37}$$

and

$$\eta = a \cos \theta + \frac{1}{2} a^2 k \cos 2\theta + \dots \tag{38}$$

Weakly nonlinear gravity waves have a phase speed greater than linear waves of the same wavelength. The effect of the higher harmonics on the shape of the waves leads to a vertical asymmetry with sharper crests and flatter troughs.

The largest such uniform wave train has a slope of $ak = 0.446$ a phase speed of $1.11c$, and a discontinuity in slope at the crest containing an included angle of 120 degrees. This limiting form has sometimes been used as the basis for the models of wave breaking; however, uniform wave trains are unstable to side-band instabilities at significantly lower slopes, and it is unlikely that this limiting form is ever achieved in the ocean.

With the assumption of both weak nonlinearity and weak dispersion (or small bandwidth, $\delta k/k_o \ll 1$), it may be shown that if,

$$\eta(x, y, t) = \Re\left[A(x, y, t)\, e^{i(k_o x - \sigma_o t)}\right] \tag{39}$$

where $\sigma_o = \sigma(k_o)$ and R means that the real part is taken, then the complex wave envelope $A(x, y, t)$ satisfies a nonlinear Schrödinger equation or one of its variants. Solutions of the nonlinear Schrödinger equation for initial conditions that decay sufficiently rapidly in space evolve into a series of envelope solitons (solitary waves) and a dispersive tail. Solitons propagate as waves of permanent form and survive interactions with other solitons with just a change of phase. Attempts have been made to describe ocean surface waves as fields of interacting envelope solitons; however, instabilities of the two-dimensional soliton solutions, and the effects of higher-order nonlinearities, random phase and amplitude fluctuations in real wave fields give pause to the applicability of these idealized theoretical results.

Resonant Interactions

Modeling the generation, propagation, interaction, and dissipation of wind-generated surface waves is of great importance for a variety of scientific, commercial, and social reasons. A rigorous theoretical foundation for all components of this problem does not yet exist, but there is a rational theory for weakly nonlinear wave–wave interactions.

For linear waves freely propagating away from a storm, the spectral content at any later time is explicitly defined by the initial storm conditions. For a nonlinear wave field, wave–wave interactions can lead to the generation of wavenumbers different from those comprising the initial disturbance. For surface gravity waves, these nonlinear effects lead to the generation of waves of lower and higher wavenumber with time. The timescale for this evolution in a random homogeneous wave field is of the order of $(ak)^4$ times a characteristic wave period; slow, but significant over the life of a storm.

The foundation of weakly nonlinear interactions between surface waves is the resonant interaction between waves satisfying the linear dispersion relationship. It is a simple consequence of quadratic nonlinearity that pairs of interacting waves lead to the generation of waves having sum and difference frequencies relative to the original waves. Thus

$$\mathbf{k}_3 = \pm\mathbf{k}_1 \pm \mathbf{k}_2, \quad \sigma_3 = \pm\sigma_1 \pm \sigma_2 \tag{40}$$

If in addition, $\sigma_i (i = 1, 2, 3)$ satisfies the dispersion relationship, then the interaction is resonant. In the case of surface waves, the nonlinearities arise from the surface boundary conditions, and resonant triads are possible for gravity capillary waves, and gravity waves in water of intermediate depth.

For deep-water gravity waves, cubic nonlinearity is required before resonance occurs between a quartet of wave components:

$$\mathbf{k}_1 \pm \mathbf{k}_2 \pm \mathbf{k}_3 \pm \mathbf{k}_4 = 0$$
$$\sigma_1 \pm \sigma_2 \pm \sigma_3 \pm \sigma_4 \ldots = 0, \quad \sigma_i = \left(gk_i\right)^{1/2} \tag{41}$$

These quartet interactions comprise the basis of nonlinear wave–wave interactions in operational models of surface gravity waves. Exact resonance is not required, since even with detuning significant energy transfer can occur across the spectrum. The formal basis of these theories may be cast as problems of multiple spatial and temporal scales, and higher-order interactions should be considered as these scales increase, and the wave slope increases.
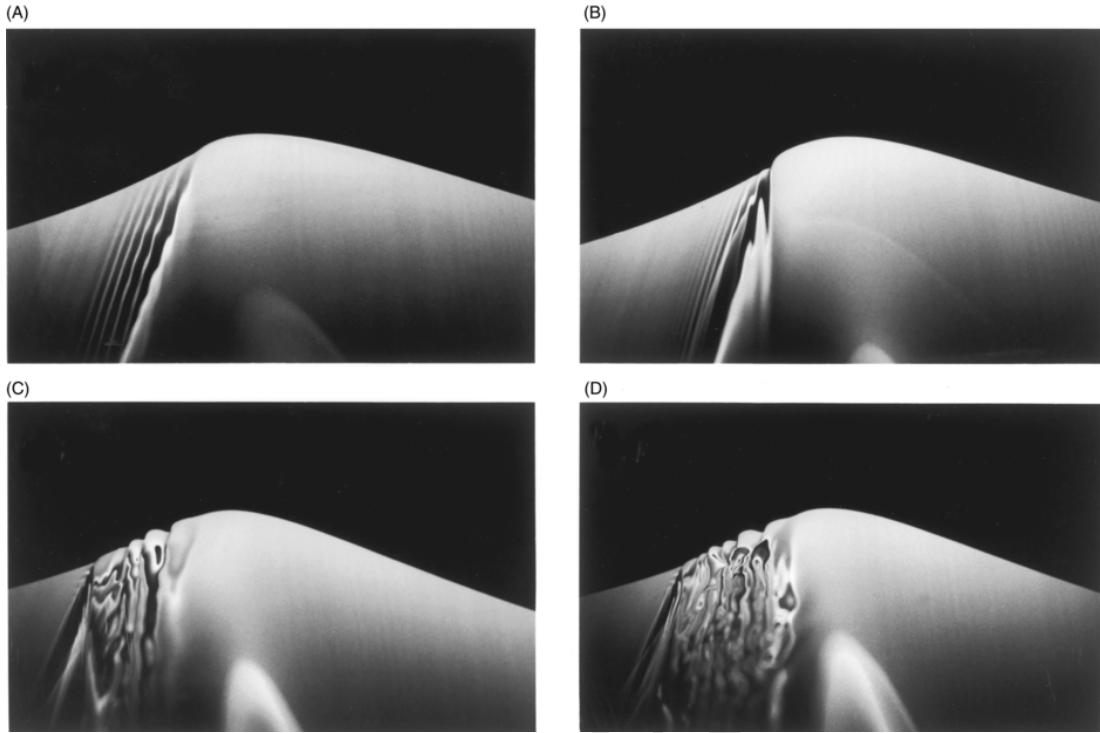
Parasitic Capillary Waves

The longer gravity waves are the dominant waves at the ocean surface, but recent developments in air–sea interaction and remote sensing, have placed increasing importance on the shorter gravity-capillary waves. Measurements of gravity-capillary waves at sea are very difficult to make and much of the detailed knowledge is based on laboratory experiments and theoretical models.

Laboratory measurements suggest that the initial generation of waves at the sea surface occurs in the gravity-capillary wave range, initially at wavelengths of $O(1)$ cm. As the waves grow and the fetch increases, the dominant waves, those at the peak of the spectrum, move into the gravity-wave range. A simple estimate of the effects of surface tension based on the surface tension parameter Σ using the gravity wavenumber k would suggest that they are unimportant, but as the wave slope increases and the curvature at the crest increases, the contribution of the Laplace pressure near the crest increases. A consequence is that so-called parasitic capillary waves may be generated on the forward face of the gravity wave (**Fig. 3**).

The source of these parasitic waves can be represented as a perturbation to the underlying gravity wave caused by the localized Laplace pressure component at the crest. This is analogous to the "fish-line" problem of Rayleigh, who showed that due to the differences in the group velocities, capillary waves are found ahead of, and gravity waves behind, a localized source in a stream. In this context the capillary waves are considered to be steady relative to the crest. The possibility of the direct resonant generation of capillary waves by perturbations moving at or near the phase speed of longer gravity waves is implied by the form of the dispersion curve in **Fig. 2**. Free surfaces of large curvature, as in parasitic capillary waves, are not irrotational and so the effects of viscosity in transporting vorticity and dissipating energy must be accounted for. Theoretical and numerical studies show that the viscous dissipation of   the   longer   gravity   waves   is   enhanced   by   one   to   two   orders   of

Fig. 3 (A–D) Evolution of a gravity wave toward breaking in the laboratory. Note the generation of parasitic capillary waves on the forward face of the crest. Reproduced with permission from Duncan, J. H. et al. (1994). The formation of a spilling breaker. *Physics of Fluids* **6**, S2.

magnitude by the presence of parasitic capillary waves. These studies also show that the observed high wavenumber cut-off in the surface wave spectrum that has been observed at wavelengths of approximately $O(10^{-3} - 10^{-2})$ m can be explained by the properties of the spectrum of parasitic capillary waves bound to short steep gravity waves.

Wave Breaking

Although weak resonant and near-resonant interactions of weakly nonlinear waves occur over slow timescales, breaking is a fast process, lasting for times comparable to the wave period. However, the turbulence and mixing due to breaking may last for a considerable time after the event. Breaking, which is a transient, two-phase, turbulent, free-surface flow, is the least understood of the surface wave processes. The energy and momentum lost from the wave field in breaking are available to generate turbulence and surface currents, respectively. The air entrained by breaking may, through the associated buoyancy force on the bubbles, be dynamically significant over times comparable to the wave period as the larger bubbles rise and escape through the surface. The sound generated with the breakup of the air into bubbles is perhaps the dominant source of high frequency sound in the ocean, and may be used diagnostically to characterize certain aspects of air–sea interaction. **Fig. 4** shows examples of breaking waves in a North Atlantic storm.

If waves break in shallow areas such as sandy beaches due to shoaling bathymetry (viz., depth-induced breaking), the dissipated wave energy and momentum are transferred to interior water to excite wave set-up and littoral currents. They are crucial to beach erosion and accretion associated with intensive sediment transport, increase of sea surface height during storm surges, and swimming safety through offshore-directed rip currents, and thus have been a central topic of nearshore oceanography and coastal engineering (e.g., **Uchiyama et al., 2010**).

Since direct measurements of breaking in the field are so difficult, much of our understanding of breaking comes from laboratory experiments and simple modeling. For example, laboratory experiments and similarity arguments suggest that the rate of energy loss per unit length of the breaking crest of a wave of phase speed c is proportional to $\rho g^{-1} c^5$, with a proportionality factor that depends on the wave slope, and perhaps other parameters. Attempts are underway to combine such simple modeling along with field measurements of the statistics of breaking fronts to give an estimate of the distribution of dissipation across the wave spectrum. Recent developments in the measurement and modeling of breaking using optical, acoustical microwave and numerical techniques hold the promise of significant progress in the next decade.
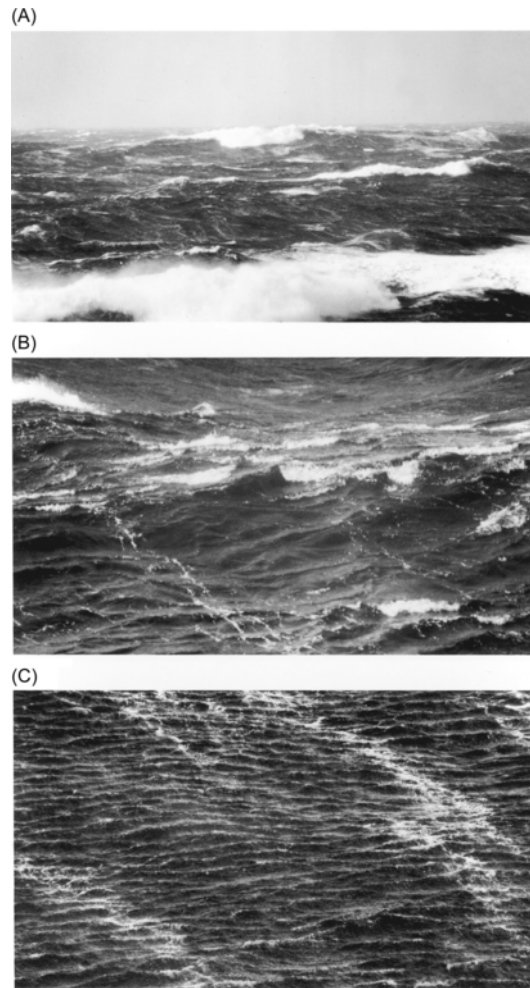
Fig. 4   Waves in a storm in the North Atlantic in December 1993 in which winds were gusting up to 50–60 knots and wave heights of 12–15 m were reported. Breaking waves are (A) large, (B) intermediate, and (C) small scale. Photographs by Terrill, E. and Melville, W. K. reproduced with permission from Melville, W.K. (1996). The role of wave breaking in air–sea interaction. *Annual Review of Fluid Mechanics* **28**, 279–321.

Further Reading

Komen, G.J., Cavaleri, L., Donelan, M., et al., 1994. Dynamics and modeling of ocean waves. Cambridge University Press, Cambridge.

Lamb, H., 1945. Hydrodynamics. Dover Publications, New York.

LeBlond, P.H., Mysak, L.A., 1978. Waves in the ocean. Elsevier, Amsterdam.

Lighthill, J., 1978. Waves in fluids. Cambridge University Press, Cambridge.

Mei, C.C., 1983. The applied dynamics of ocean surface waves. John Wiley, New York.

Melville, W.K., 1996. The role of wave breaking in air–sea interaction. Annual Review of Fluid Mechanics 28, 279–321.

Phillips, O.M., 1977. The dynamics of the upper ocean. Cambridge University Press, Cambridge.

Uchiyama, Y., McWilliams, J.C., Shchepetkin, A.F., 2010. Wave-current interaction in an oceanic circulation model with a vortex force formalism: Application to the surf zone. Ocean Modeling 34 (1–2), 16–35.

Whitham, G.B., 1974. Linear and nonlinear waves. John Wiley, New York.

Yuen, H.C., Lake, B.M., 1980. Instability of waves on deep water. Annual Review of Fluid Mechanics 12, 303–334.